RESEARCH ARTICLE
doi: 10.2306/scienceasia1513-1874.2025.029

ScienceAsia 51 (2): 2025: ID 2025029: **1–11**

LncRNA MALAT1 promoted PA-induced damage and reduced insulin secretion in MIN6 cells through Phospho-p38 pathway

Yang Ou[a], **Jiaxin Liu**[b], **Chao Liu**[c], **Zhongxiong Zheng**[a], **Heng Su**[a,*]

[a] Department of Endocrinology and Metabolism, First People's Hospital of Yunnan Province (The Affiliated Hospital of Kunming University of Science and Technology), Kunming 650032 China
[b] School of Medicine, Kunming University of Science and Technology, Kunming 650500 China
[c] Department of General Affairs, First People's Hospital of Yunnan Province (The Affiliated Hospital of Kunming University of Science and Technology), Kunming 650032 China

*Corresponding author, e-mail: su_hen@hotmail.com

Received 5 Jun 2024, Accepted 2 Jan 2025
Available online 1 May 2025

ABSTRACT: This study aimed to investigate the role of LncRNA MALAT1 in pancreatic β-cell dysfunction in type 2 diabetes mellitus (T2DM) and its mechanisms, particularly focusing on the Phospho-p38 signaling pathway. MIN6 cells were treated with palmitic acid (PA) to induce β-cell dysfunction. Transcriptome analysis revealed upregulation of LncRNA MALAT1, which was further investigated for its effects on cell proliferation, apoptosis, ROS production, and insulin secretion. The involvement of the Phospho-p38 signaling pathway was explored through rescue experiments using DHC, an activator of Phospho-p38. *In vivo* validation was conducted using a T2DM rat model. PA treatment reduced cell proliferation, increased apoptosis, elevated ROS, and decreased insulin secretion. Knockdown of MALAT1 improved these dysfunctions and downregulated the Phospho-p38 pathway. *In vivo* studies confirmed the upregulation of MALAT1 and Phospho-p38 alongside significant β-cell dysfunction. This study demonstrated that LncRNA MALAT1 played a crucial role in pancreatic β-cell dysfunction in T2DM by activating the Phospho-p38 signaling pathway. Knockdown of MALAT1 mitigated PA-induced β-cell damage by downregulating Phospho-p38, highlighting the MALAT1/Phospho-p38 axis as a potential therapeutic target for preserving pancreatic β-cell function in T2DM. These findings provide new insights into the molecular mechanisms underlying T2DM and suggest novel avenues for intervention.

KEYWORDS: pancreatic β-cell dysfunction, LncRNA MALAT1, Phospho-p38, MIN6, T2DM rat model

INTRODUCTION

T2DM is a metabolic disease characterized by insulin secretion deficiency and impaired insulin action in peripheral tissues. The primary defect in T2DM is the dysfunction of pancreatic β-cells, which fail to respond to glucose stimulation by adequately secreting insulin. To investigate the pathological mechanisms underlying T2DM, researchers often utilize pancreatic β-cell lines such as MIN6 cells, exposing them to high glucose or high fatty acid (e.g., PA) environments to simulate β-cell dysfunction [1]. In recent years, research has found that T2DM is closely related to changes in lncRNA [2] and protein phosphorylation [3]. For instance, in normal glucose metabolism, LINC317.5 has been identified as a novel biomarker for hypertriglyceridemia [4]. LncRNA NEAT1 plays a regulatory role in the progression of T2DM accompanied by obstructive sleep apnea [5]. Additionally, the phosphorylation levels of proteins such as TGR5, PKA, and CREB are associated with the microbiota in T2DM [6], and the phosphorylation level of Tau protein is related to metabolic disorders and neuropsychiatric damage in type 2 diabetic mice [7]. However, the mechanism by which lncRNAs regulate protein phosphorylation levels in T2DM remains unclear.

LncRNA MALAT1 is a widely studied long non-coding RNA that plays a regulatory role in various diseases such as colitis, cardiovascular diseases, and cancers [8]. It has been identified as a new marker for the diagnosis of diabetic nephropathy [9]. Additionally, blocking the LncRNA MALAT1/miR-224-5p/NLRP3 axis inhibits the hippocampal inflammatory response in type 2 diabetes mellitus (T2DM) with obstructive sleep apnea (OSA) [10]. Phospho-p38 is a phosphorylated protein kinase that plays a key role in cellular stress responses. Studies have shown that Phospho-p38 is upregulated in the placental tissue of gestational diabetes mellitus [11], and high-fat diets promote the activation of MAPK pathways, including p-JNK and Phospho-p38 [12]. The interactions between lncRNAs and phosphorylated proteins in cellular function regulation are complex. LncRNAs can influence protein phosphorylation states through various mechanisms. For example, silencing lncRNA GAS5 enhances the activation of the phosphoinositide 3-kinase (PI3K)/protein kinase B pathway (AKT), thereby reducing myocardial injury [13]. Overexpression of lncRNA uc.134 upregulates the phosphorylation level of YAP at Ser127, thus activating Hippo signaling and promoting HCC progression [14]. However, the specific mechanisms of MALAT1 and Phospho-p38 in

T2DM are still unclear.

Animal models of T2DM are important tools for studying the pathogenesis and treatment strategies of T2DM [15]. Commonly used T2DM animal models include those induced by a high-fat, high-sugar diet combined with low-dose STZ. These models effectively simulate the metabolic characteristics of T2DM, such as insulin resistance and β-cell dysfunction, thereby aiding in the understanding of the complex pathological processes of T2DM [16]. By integrating cell and animal models, the regulatory mechanisms of MALAT1 and Phospho-p38 in T2DM could be more comprehensively analyzed and, hence, provide a theoretical basis for developing new therapeutic strategies.

MATERIALS AND METHODS

Construction of a rat model of diabetes mellitus

This study involved 8-week-old male Sprague-Dawley rats (200 ± 20 g) obtained from HFK Biotechnology (Beijing, China). After a one-week acclimatization period, the rats were randomly assigned to either a normal control (NC) group or a T2DM group. There were five male rats in each group. The NC group received a standard diet, while the T2DM group was fed a high-fat diet (HFD, XieTong, China) consisting of 60% kcal from fat, 20% kcal from carbohydrates, and 20% kcal from protein. After 4 weeks on their respective diets, all animals were fasted overnight. STZ (MCE, USA) was dissolved in freshly prepared cold 0.1 M citrate buffer (pH 4.5) (MCE) to a final concentration of 40 mg/ml. The solution was kept on ice and protected from light due to STZ's photosensitivity. The T2DM group was injected with a single tail vein injection of STZ at a dose of 30 mg/kg, while the NC group was injected with the same dose of the buffer carrier. After injecting streptozotocin, fasting plasma glucose (FPG) levels were measured on days 3, 9, and 14. Fasting blood glucose (FBG) levels exceeding 16.8 mmol/l were considered successfully induced diabetic. All animal experiments were approved by the Animal Ethics Committee of Kunming University of Science and Technology (Kmust-MEC-2023-014). All animal experiments were performed following the institutional guidelines for the humane treatment of animals, the Principles of Laboratory Animal Care (National Institutes of Health, Bethesda, MD, USA) (https://www.ncbi.nlm.nih.gov/books/NBK54050).

Oral glucose tolerance test

The test started by fasting the rats for 12 h overnight, ensuring they had access to water but no food. After the fasting period, a baseline blood sample from the tail vein of each rat was collected, and the FBG level was measured using a glucometer (Roche, USA). A glucose solution (Beyotime, China) was prepared at a concentration allowing an administration of a 2 g/kg body weight dose to be delivered orally using a gavage needle (Yuyan, China). Following the glucose administration, BGLs were measured at multiple time points: 30 min, 60 min, 90 min, and 120 min post-gavage. At each time point, blood samples were collected from the tail vein for glucose concentration measurement using a glucometer, and the area under the curve (AUC) for the glucose levels over the 120-min period were calculated to assess glucose tolerance in each rat.

Cell culture and treatment

To culture MIN6 cells, please refer to our previous articles [14]. The MIN6 cell line, obtained from the BeNa Culture Collection (China), was subjected to 18 rounds of cell passage. The Cells were cultured in Dulbecco's Modified Eagle's Medium (DMEM, Gibco, USA), supplemented with 15% fetal bovine serum (FBS, Gibco) and 1% penicillin-streptomycin solution (Penicillin-Streptomycin, Gibco) at 37 °C in a 5% CO_2 incubator (Thermo Fisher Scientific, USA). The cells were regularly monitored for changes of morphology and growth, and the medium was changed every 2 to 3 days. When the cell density reached 80%–90%, they were passaged or split. Based on the experimental design, the cells were seeded in 6-well or 96-well plates, continued culturing until they reach 60% confluence, then proceeded with the drug treatment. Cells in the PA group were exposed to 400 μM PA for 24 h, while those in the PA+DHC group were pretreated with 10 μg/ml DHC for 2 h before PA addition. After removing the old medium, the cells were washed twice with PBS and glucose-free KRBH buffer containing 0.1% BSA and, then, incubated for 60 min at 37 °C and 5% CO_2 in an incubator. After the incubation, the cells were cultured in DMEM containing 25 mM glucose for 60 min. Subsequent cell experiments were biologically repeated three times.

Transcriptome sequencing analysis

This study conducted transcriptome sequencing on cells of the NC and the PA groups (400 μM PA + 25 mM glucose) performed by LC-Bio. Cells were collected, quickly frozen in liquid nitrogen, and stored at −80 °C. RNA was extracted using TRIzol reagent, with concentration and purity measured by NanoDrop (A260/A280 ratio between 1.8–2.0); and RNA integrity was assessed using the Agilent 2100 Bioanalyzer (RIN > 7.0). The rRNA was depleted to focus on mRNA and lncRNA, followed by cDNA synthesis and library construction using the Illumina TruSeq RNA Sample Preparation Kit. Sequencing was performed on the Illumina HiSeq 2500 platform with 150 bp paired-end reads, targeting at least 30–50 million reads per sample. FastQC performed quality control on the raw data, filtered low-quality reads, and trimmed the adapter sequence. Cleaned reads were aligned to the reference genome using HISAT2, and transcripts were assembled with StringTie. Gene expression was quan-

tified using FeatureCounts, yielding raw count data for each lncRNA. Normalization of raw counts was done using TPM methods, and differential expression analysis was performed with DESeq2, applying a criterion of $p < 0.05$ and $|\log2(fc)| > 2$. A generalized linear model (GLM) was fitted to the normalized counts, with hypothesis testing identifying lncRNAs with significant expression changes. The Benjamini-Hochberg procedure was used for multiple testing corrections. Differential genes were visualized with heatmaps.

Cell transfection

The lentiviral vectors carrying sh-LncRNA MALAT1 (HanHeng, China) were named sh-LncRNA MALAT1-1, sh-LncRNA MALAT1-2, and sh-LncRNA MALAT1-3. The viral titer was 10^8 TU/ml. The lentivirus expressing LncRNA MALAT1 was diluted in complete DMEM without antibiotics. To enhance transduction efficiency, 8 µg/ml polybrene was added to the medium. Transfection was performed when the cells reached 80% confluence. The original medium was removed from the cells, and the medium containing the virus was added. The cells were incubated for 4–6 h in an incubator at 37 °C and 5% CO_2. After incubation, the virus-containing medium was replaced with the puromycin-containing medium. In order to confirm the transfection efficiency of the LncRNA MALAT1 lentivirus, qPCR was used to detect LncRNA MALAT1 expression.

Western blotting

Cells were washed with cold PBS (Beyotime) and incubated in cold RIPA lysis buffer (Thermo Fisher Scientific) with a cocktail of protease and phosphatase inhibitors, followed by sonication for 10 s. Cell lysates were centrifuged at 12,000×g for 10 min at 4 °C; and protein concentration was quantified using the PierceTM BCA Protein Assay Kit (Thermo Fisher Scientific) according to the manufacturer's protocol. An equal amount of protein lysates was separated by sodium dodecyl sulfate–polyacrylamide gel electrophoresis (SDS-PAGE) and transferred onto nitrocellulose membranes. The membranes were blocked with 5% BSA prepared in TBST for 1 h at room temperature and then probed overnight at 4 °C with the respective primary antibodies. After washing, the membranes were incubated with horseradish peroxidase (HRP)-conjugated secondary antibodies in TBST containing 5% BSA for 1 h at room temperature. HRP-conjugated secondary antibodies were used to detect protein expression using chemiluminescence. ImageJ software was used to perform densitometry on scanned immunoblot images.

CCK-8

MIN6 cells (1×10^5 cells/well) were inoculated into 96-well plates. MIN6 cells were stimulated with 0.4 mmol/L PA and 25 mM glucose for 24 h. Ten µl CCK-8 reagent (Dojindo, Japan) was added to each well, and the plates were incubated at 37 °C for 3 h. Absorbance was then measured at 450 nm using an enzyme marker. The experiment was performed in triplicate.

Apoptosis assay

Following the grouping information, the cells were processed and analyzed for MIN6 apoptosis using the Membrane Linked Protein V-FITC Apoptosis Detection Kit (BD Biosciences, USA). The cell suspension was added with 5 µl Annexin V-APC and 5 µl PI dye after digestion of the cells with trypsin and incubated for 1 h at room temperature; then, cell apoptosis was detected using a CytoFLEX S flow cytometer (Beckman Coulter, USA).

ELISA

ELISA kit (MlBIO, China) and mouse serum insulin detection kit (Tongwei, China) were used to detect insulin levels in cell supernatants and rat serum, respectively.

Quantitative PCR

Total RNA was isolated from MIN6 cells with Eastep® Super Total RNA reagent (Promega, USA) according to the supplier's instructions. The operation method was detailed in our previous article [14]. The PCR primers were synthesized by Takara Bio, and the sequences were as follows: LncRNA Pvt1 forward: 5′-ACCTCCTCCCTTCTTTCTCATCAG-3′, reverse: 5′-TCACACTCGCTCCTTCACACTC-3′; LncRNA MALAT1 forward: 5′-CATACGGATGTGGTGGTGAAGC-3′, reverse: 5′-AATGCCTGCTCGCCTCCTC-3′; LncRNA Dleu2 forward: CGCTACACCGACTGACATTTACC, reverse: 5′-TGCTCTGGAAGAACACTGATTGG-3′; and GAPDH forward: 5′-GGTTGTCTCCTGCGACTTCA-3′, reverse: 5′-TGGTCCAGGGTTTCTTACTCC-3′. Three technical replicates were performed and $2^{\Delta\Delta CT}$ method was adopted for data analysis.

Measurement of reactive oxygen species (ROS)

Intracellular ROS was measured by measuring the fluorescence intensity of 2′,7′-dichlorofluorescein (DCF). Cells were stained with 15 µM dichlorodihydrofluorescein diacetate (DCFH-DA, Applygen, China) for 37 min. Then, the cells were washed twice with PBS. Fluorescence was measured, using a fluorescence microscope (Olympus IX81, Japan) at the excitation wavelength of 488 nm and the emission wavelength of 525 nm, and photographed.

Hematoxylin and eosin (HE) staining

After the T2DM model was successfully established, the pancreatic tissue was fixed with 4% paraformaldehyde at room temperature, and 5 µm thick paraffin

sections were made. The sections were deparaffinized to water, and then stained with hematoxylin and eosin (H&E) (Solarbio, China). For H&E staining, the sections were stained by hematoxylin lasting 5 min, and differentiated by hydrochloric acid ethanol at room temperature for 3 s. After returning to blue by rinsing with tap water for 30 min, the sections were counterstained with eosin staining solution for 2 min. Finally, the morphological changes of pancreatic tissue were observed by microscope (Nikon, Japan).

Statistical analysis

Each experiment was conducted with repetitions, including three replicates for cell experiments and five replicates for animal experiments. Data were expressed as mean ± standard deviation (SD). Comparisons between the two groups were performed using the Student's *t*-test, chosen for its ability to assess statistically significant differences between the means of two independent groups. For comparisons among three or more groups, one-way ANOVA followed by Tukey's post hoc test was utilized. This approach allowed for the detection of differences among multiple groups while controlling for type I errors, ensuring that research questions were appropriately addressed by the analysis. Statistical significance was set at $p < 0.05$. All analyses were conducted using GraphPad Prism Version 6 (GraphPad).

RESULTS

Modeling β-cell dysfunction in T2DM: PA-induced damage in MIN6 cells

The pathogenesis of T2DM is closely associated with pancreatic β-cell dysfunction [1]. To model this dysfunction in T2DM, we selected MIN6 cells as our research model. Dysfunction in MIN6 cells was induced using PA. Following the PA induction, MIN6 cells exhibited reduced proliferation (Fig. 1B), increased apoptosis (Fig. 1C), and elevated ROS production (Fig. 1D), indicating significant cellular damage. Additionally, the reduction in insulin secretion (Fig. 1A) further confirmed the impairment of insulin function. These results successfully mimicked the pathological process of β-cell dysfunction observed in T2DM.

Effects of PA induction on LncRNA expression in MIN6 cells

T2DM, a prevalent chronic metabolic disease, is influenced by multiple factors [1]. Researches indicate that LncRNAs are involved in regulating pancreatic β-cell function, but the specific LncRNAs responsible for this regulation remain unclear. To investigate this, we performed transcriptome analysis on normal MIN6 pancreatic β-cells and PA-induced dysfunctional MIN6 cells to identify changes in LncRNA expression within the β-cells. The results showed that, compared with the NC group, 17 lncRNAs were downregulated, and 25 lncRNAs were upregulated in the PA group (Fig. 2A). Based on a literature review, we selected three diabetes-related genes for validation: LncRNA Dleu2, LncRNA MALAT1, and LncRNA PVT1. The results indicated that LncRNA Dleu2 was downregulated in the PA group, while LncRNA MALAT1 and LncRNA PVT1 were significantly upregulated, with the upregulation of LncRNA MALAT1 being more pronounced than that of the LncRNA PVT1 (Fig. 2B). In subsequent experiments, we selected LncRNA MALAT1 as the target for studying β-cell dysfunction in T2DM.

Knockdown of LncRNA MALAT1 improved PA-induced islet cell damage and restored cell function

To investigate the impact of LncRNA MALAT1 on β-cell dysfunction in T2DM, we knocked down MALAT1 and assessed the knockdown efficiency using RT-qPCR. We designed three short hairpin RNA (shRNA) sequences targeting MALAT1 — sh-MALAT1 1, sh-MALAT1 2, and sh-MALAT1 3 — as experimental groups. The control group consisted of cells transfected with sh-control viral particles. The results showed that sh-MALAT1 2 significantly reduced MALAT1 expression in MIN6 cells (Fig. 3A), leading us to select sh-MALAT1 2 for further study. Knockdown of MALAT1 enhanced cell proliferation (Fig. 3C), reduced apoptosis (Fig. 3D), and decreased ROS production (Fig. 3E). These findings suggested that inhibiting MALAT1 expression in T2DM could mitigate PA-induced damage in MIN6 cells. Additionally, suppressing MALAT1 expression in T2DM promoted insulin secretion (Fig. 3B) in MIN6 cells, indicating that MALAT1 played a role in regulating islet function, and its inhibition might rescue β-cell dysfunction.

MALAT1 knockdown mitigated PA-induced β-cell dysfunction in T2DM by downregulating Phospho-p38 pathway

To investigate how LncRNA MALAT1 affecting β-cell dysfunction in T2DM through Phospho-p38, we first assessed the protein expression levels of Phospho-p38 and p38 following PA induction. The results showed that PA significantly increased Phospho-p38 expression (Fig. 4A). Next, we examined the impact of MALAT1 knockdown on the expression of Phospho-p38 and p38 proteins, using DHC to activate Phospho-p38 as a rescue experiment. The findings revealed that DHC upregulated Phospho-p38 protein levels, while MALAT1 knockdown reduced Phospho-p38 expression in both the presence and the absence of DHC (Fig. 4B). QPCR analysis of LncRNA MALAT1 expression indicated that MALAT1 knockdown led to a decrease in its expression regardless of DHC treatment, whereas DHC treatment alone did not significantly alter LncRNA MALAT1 expression levels (Fig. 4C). These results suggested that while MALAT1 knockdown downregulates Phospho-

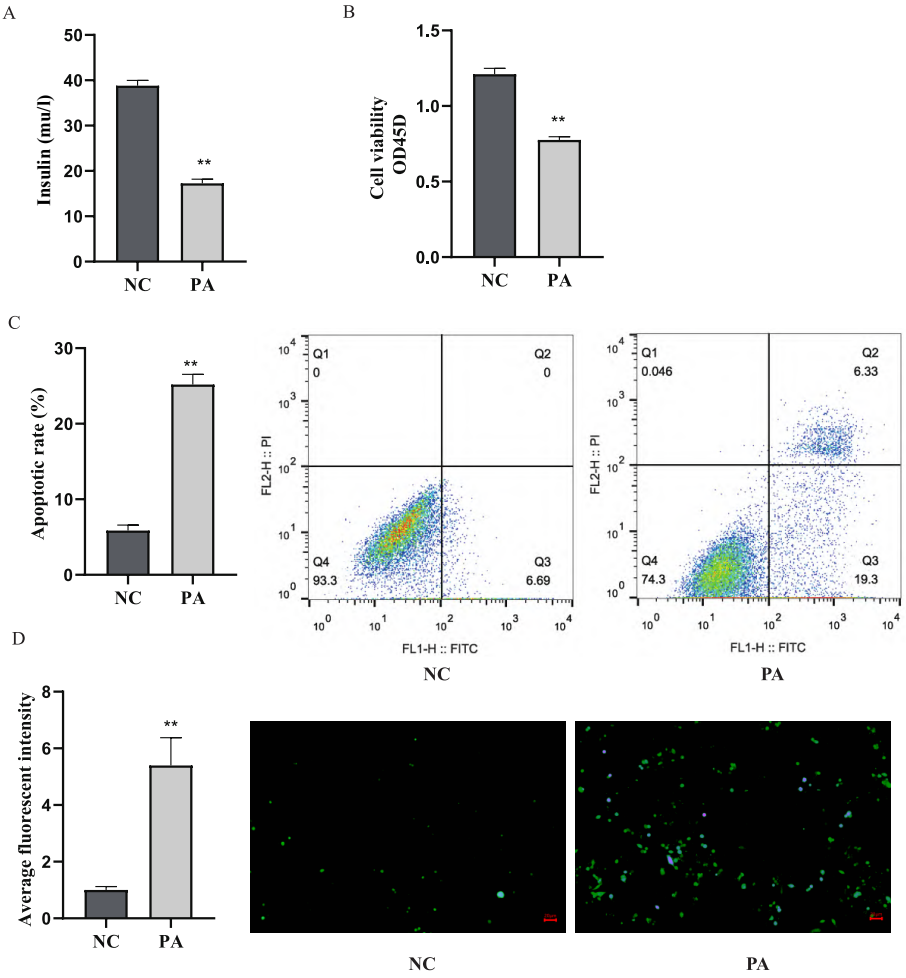

Fig. 1 Modeling β-cell dysfunction in T2DM: PA-induced damage in MIN6 cells. MIN6 cells were incubated with 400 μM PA for 24 h to construct a T2DM cell model: A, ELISA was performed to determine the insulin level to evaluate whether the modeling was successful; B, cell viability assessed by CCK-8 assay; C, cell apoptosis detected by flow cytometry; D, ROS levels detected by immunofluorescence. All values are mean ± SD ($n = 3$ biological replicates). ** $p < 0.01$ vs. NC group.

p38, the activation of Phospho-p38 does not affect MALAT1 expression. Furthermore, we found that DHC treatment inhibited insulin secretion (Fig. 4D), reduced cell proliferation (Fig. 4E), increased apoptosis (Fig. 4F), and elevated ROS production (Fig. 4G). Notably, MALAT1 knockdown reversed the DHC-induced reduction in insulin secretion, decreased cell proliferation, increased apoptosis, and elevated ROS levels (Fig. 4D–G). These findings suggested that MALAT1 knockdown mitigates PA-induced β-cell dysfunction in T2DM by downregulating Phospho-p38.

Upregulation of LncRNA MALAT1 and Phospho-p38 in a T2DM rat model

To verify the *in vivo* expression of LncRNA MALAT1 and Phospho-p38, we successfully established a T2DM rat model and conducted relevant analyses. In the control group, the pancreatic islet cells were neatly arranged, and the boundaries between the islets and surrounding tissues were visible. In contrast, the T2DM group showed significant pancreatic tissue damage, characterized by islet atrophy, inflammatory cell infiltration, and disordered islet cell arrangement (Fig. 5A). ELISA analysis revealed that serum insulin levels in the T2DM group were significantly lower than those in the control group (Fig. 5B), indicating impaired β-cell function. The T2DM rats also exhibited significantly higher levels of triglycerides (TG), total cholesterol (TC), and low-density lipoprotein cholesterol (LDL-C); while high-density lipoprotein cholesterol (HDL-C) levels were significantly reduced (Table S1), reflecting the adverse impact of diabetes on lipid metabolism. Blood glucose levels in the T2DM group were markedly elevated (Fig. 5C), further confirming the successful establishment of the T2DM model. These results indicate that we successfully simulated T2DM-induced β-cell

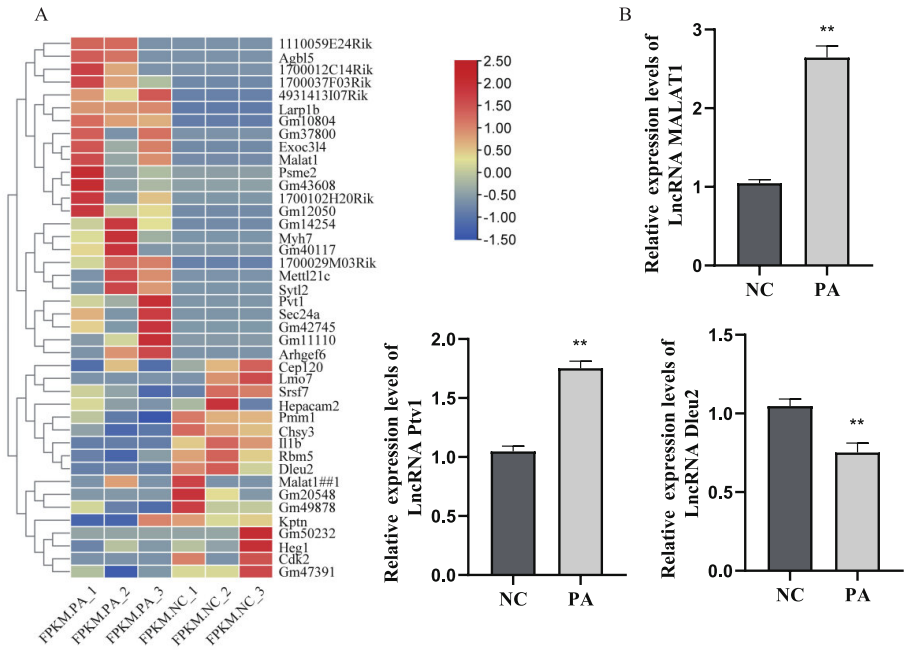

Fig. 2 Effects of PA induction on LncRNA expression in MIN6 cells. MIN6 cells were incubated with 400 μM PA for 24 h to construct a T2DM cell model. A, The heatmap displaying gene expression levels in cells of the NC and PA groups. Gene expression was shown using log10(FPKM+1), with the x-axis representing samples and the y-axis representing genes. Different colors indicate different levels of gene expression, with the color gradient ranging from blue through white to red, representing expression levels (log10(FPKM+1)) from low to high. Red indicates high-expression genes, while dark blue indicates low-expression genes. B, RT-qPCR detection of LncRNA Dleu2, LncRNA MALAT1, and LncRNA PVT1 expressions. All values are mean ± SD ($n = 3$ biological replicates). ** $p < 0.01$ vs. NC group.

dysfunction in rats. Subsequently, we analyzed the expression levels of LncRNA MALAT1 and Phospho-p38 in the context of β-cell dysfunction, and the results showed that both were significantly upregulated in the T2DM group (Fig. 5D), suggesting that they might play critical roles in T2DM-related islet dysfunction.

DISCUSSION

T2DM is a metabolic disorder influenced by both genetic factors and various external risk factors. These factors often lead to the impairment or death of pancreatic β-cells, especially under conditions of hyperglycemia, elevated free fatty acids, inflammatory factors, H2O2, and PA [17]. PA, a type of free fatty acid, is widely studied as a model for inducing β-cell damage, such as in MIN6 cells [18]. PA induces damage to MIN6 cells primarily through oxidative stress. It increases the generation of reactive oxygen species (ROS) within these cells, leading to oxidative stress. Excess ROS can cause damage to proteins, lipids, and DNA, ultimately resulting in cell dysfunction and apoptosis. Additionally, high concentrations of PA can damage the MIN6 cell membrane, causing lipotoxicity. Lipotoxicity promotes the accumulation of lipids within MIN6 cells, leading to structural damage and impaired insulin secretion [19]. Studies have shown that PA treatment reduces insulin secretion in INS-1 cells compared with controls. In C57BL/6J mice, PA administered for two weeks reduces glucose-stimulated insulin secretion (GSIS) [20]. Furthermore, PA treatment for 24 h impairs both cell viability and insulin secretion in INS-1E rat insulinoma cells and primary pancreatic islet cells [21]. PA also severely impairs GSIS in INS-1 cells in a time-dependent manner [22], with PA-induced lipotoxicity further reducing insulin secretion [23]. Additionally, PA-induced T2DM cell models exhibit increased ROS levels [24]. These findings indicate that PA not only inhibits insulin secretion but also increases cell apoptosis and ROS levels, aligning with our results. STZ is commonly used to induce diabetes in rats and mice. It induces β-cell dysfunction by reducing glucose oxidation and decreasing insulin biosynthesis and secretion. After STZ treatment, plasma insulin levels in these animal models decrease, signaling the onset of diabetes [25]. Our study similarly showed reduced serum insulin secretion and elevated blood glucose levels in T2DM rats.

LncRNA MALAT1 is a highly conserved long non-coding RNA that is closely associated with various pathological processes related to diabetes complica-

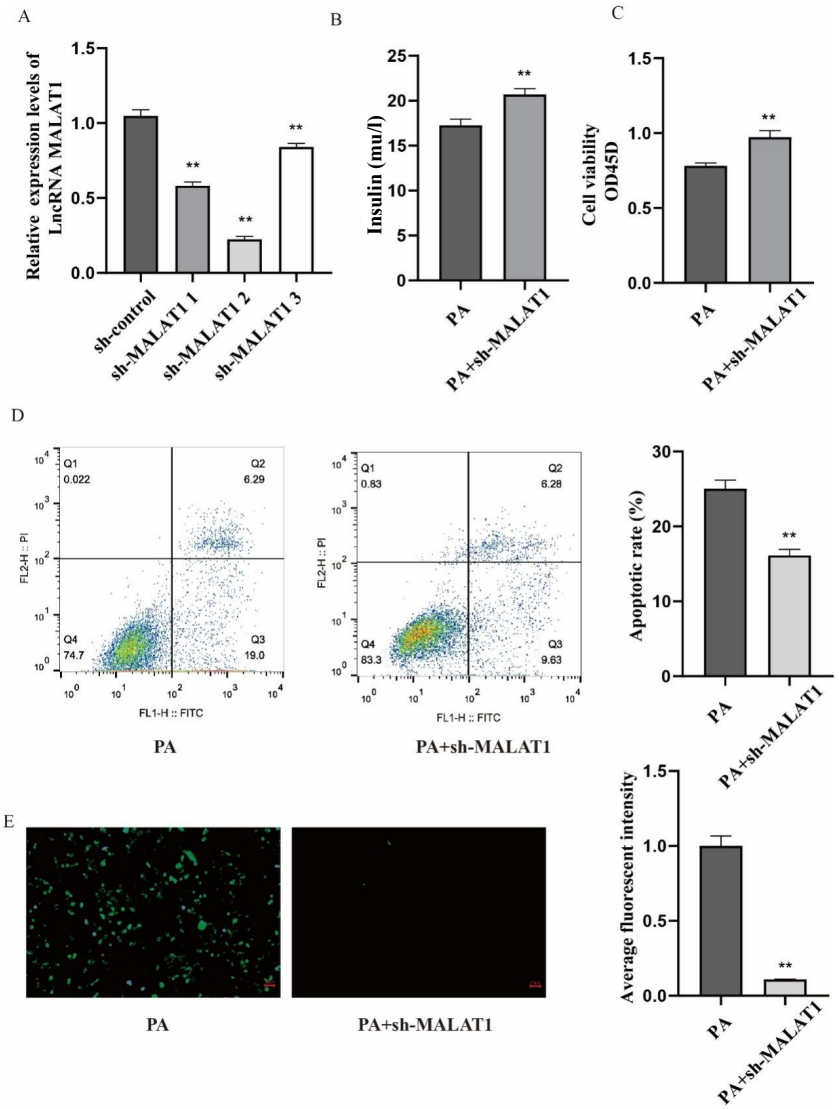

Fig. 3 Knockdown of LncRNA MALAT1 improved PA-induced islet cell damage and restored cell function. PA+sh-MALAT1 group: After PA induction to establish a T2DM model in MIN6 cells, we transfected them with lentiviral vectors carrying sh-LncRNA MALAT1: A, RT-qPCR detection of LncRNA MALAT1 expression; B, insulin secretion detected by ELISA; C; cell viability assessed by CCK-8 assay; D, cell apoptosis detected by flow cytometry; and E, ROS levels detected by immunofluorescence. All values are mean ± SD ($n = 3$ biological replicates). ** $p < 0.01$ vs. PA group.

tions and malignant tumors [26]. Studies have shown that inhibiting LncRNA MALAT1 can protect the retina from oxidative damage, preventing or slowing down diabetic retinopathy [27]. Additionally, the elevation of LncRNA MALAT1 can cause endothelial cell dysfunction and promote angiogenesis [28]. However, the impact of LncRNA MALAT1 on PA-induced MIN6 cells remains unclear. In this study, we screened the differential expression of LncRNA MALAT1 in PA-induced MIN6 cells through transcriptome sequencing. RT-qPCR validation of differentially expressed genes showed that LncRNA MALAT1 was significantly elevated in MIN6 cells, which was similar to the results in the T2DM rat group. Inhibiting LncRNA MALAT1 could increase cell viability and inhibit cell apoptosis. Furthermore, inhibiting LncRNA MALAT1 reduced the production of ROS and promoted insulin secretion in MIN6 cells.

In this study, we identified several lncRNAs, through transcriptome analysis, that have not been extensively studied in the context of diabetes. While these lncRNAs are known to play significant roles in the development and progression of various diseases, including cancer, cardiovascular diseases, and metabolic disorders [29–31], their specific functions in diabetes remain unclear. lncRNAs can influence

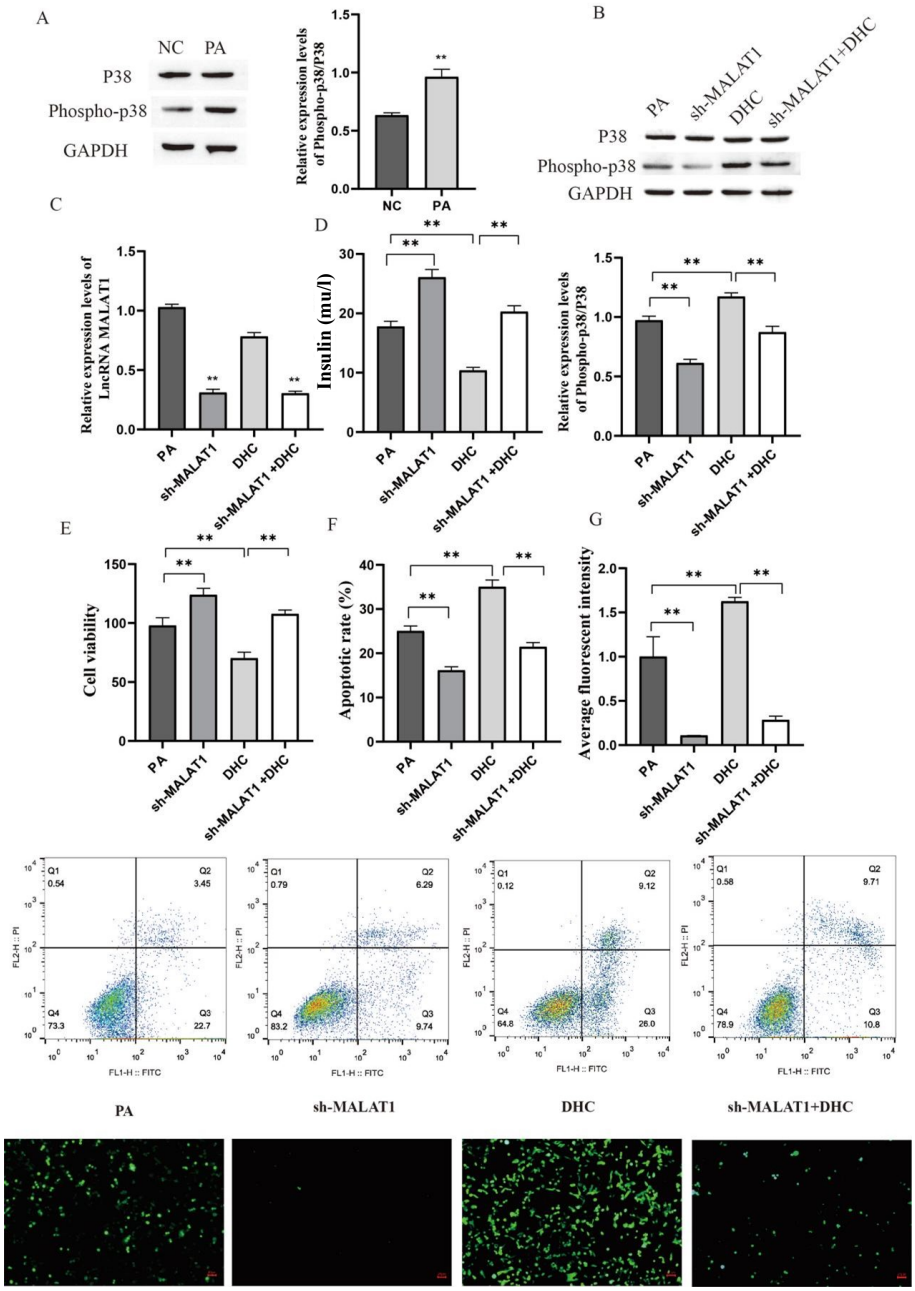

Fig. 4 MALAT1 knockdown mitigates PA-induced β-cell dysfunction in T2DM by downregulating Phospho-p38 pathway. PA+DHC group: MIN6 cells pretreated with 10 μg/ml DHC for 2 h before PA addition; PA+DHC+sh-MALAT1 group: MIN6 cells were pretreated with 10 μg/ml DHC for 2 h, then treated with PA for 24 h, and transfected with lentiviral vectors carrying sh-LncRNA MALAT1. (A,B), Western blotting detection of Phospho-p38 protein expression levels; C, RT-qPCR detection of LncRNA MALAT1 expression; D, insulin secretion detected by ELISA; E, cell viability assessed by CCK-8 assay; F, cell apoptosis detected by flow cytometry; G, ROS levels detected by immunofluorescence. All values are mean ± SD ($n = 3$ biological replicates). ** $p < 0.01$ vs. PA group; ** $p < 0.01$ vs. PA+sh-MALAT1 group.

cellular functions through multiple mechanisms, such as regulating gene expression, modulating the cell cycle, promoting or inhibiting apoptosis, and controlling cellular metabolism [32]. Our findings suggested that the upregulated lncRNAs might be linked to cellular stress responses, potentially contributing to antioxidative processes, anti-apoptotic effects, and enhanced metabolic activity [29, 30, 33]. On the other hand, the

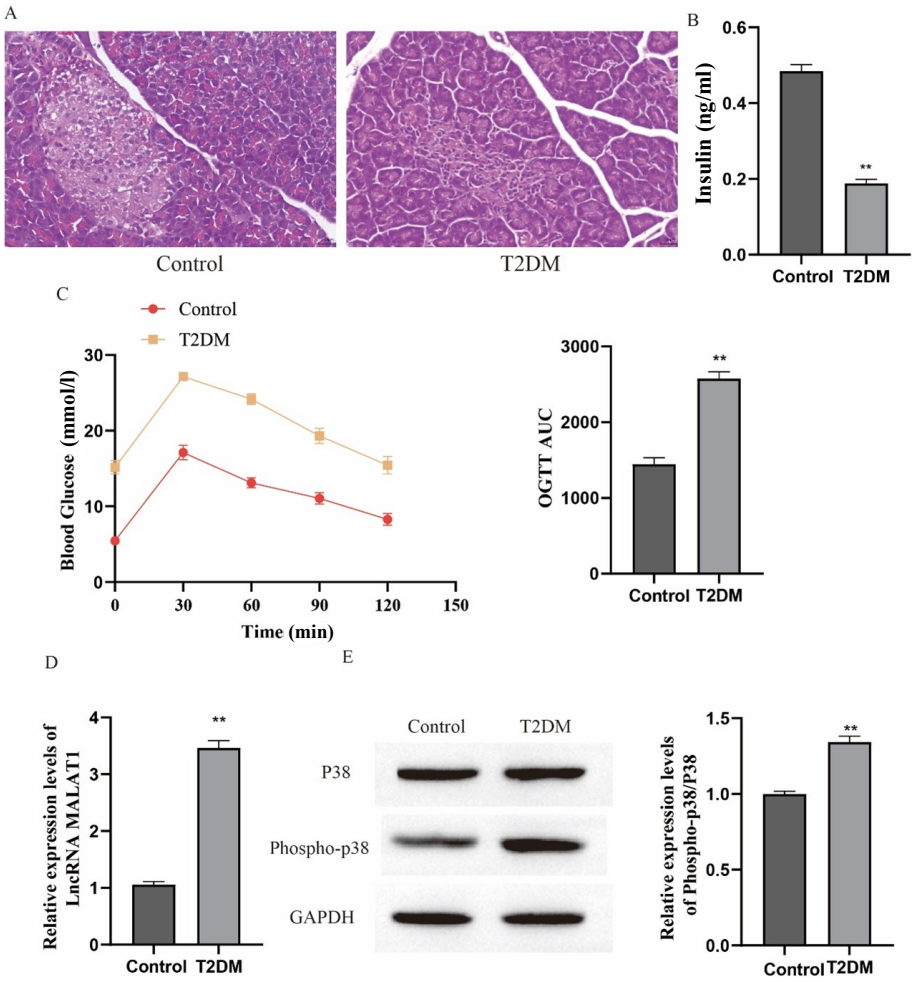

Fig. 5 Upregulation of LncRNA MALAT1 and Phospho-p38 expression in a T2DM rat model. A, HE staining; B, ELISA assay for insulin secretion; C, glucose tolerance evaluated by examining levels of blood glucose at 0, 30, 60, 90, and 120 min and AUC after oral glucose administration; D, RT-qPCR detection of LncRNA MALAT1 expression; and E, Western blotting detection of Phospho-p38 protein expression levels. All values are expressed as mean ± SD ($n = 5$ biological replicates). ** $p < 0.01$ vs. Control.

downregulated lncRNAs might lead to the suppression of protective cellular mechanisms, such as reduced cell proliferation, decreased metabolic efficiency, and diminished capacity to handle stress [34, 35]. These changes likely reflect the complex response mechanisms of MIN6 cells to PA-induced damage and highlight new potential targets for diabetes research.

The p38 MAPK signaling pathway is widely activated under various environmental and cellular stress conditions, characterized by elevated levels of phosphorylated p38 [36]. Studies have shown that palmitic acid (PA) can induce the upregulation of phosphorylated p38 protein in stem cells [37]. Furthermore, dexmedetomidine inhibits phosphorylated p38, promotes hyperglucose-induced trophoblast proliferation, and attenuates insulin resistance [38]. Our study further confirmed that PA can upregulate the expression levels of phosphorylated p38, and we also discovered that LncRNA MALAT1 regulates the expression of phosphorylated p38.

Previous research demonstrated that in high-glucose-induced human lens epithelial cells, elevated glucose levels increased oxidative stress, thereby activating various transcription factors, including SP1, which subsequently bound to the promoter region of MALAT1, enhancing its transcription. The upregulation of MALAT1 leads to increased apoptosis and oxidative stress in lens epithelial cells by activating the p38 MAPK signaling pathway [39].

Additionally, a study by J-Y Liu et al [40] found that pre-treating RF/6A cells with SB203580, a p38 activity inhibitor, significantly blocked MALAT1-induced cell proliferation. In contrast, ERK inhibitor U0126 and JNK inhibitor SP600125 did not affect the cell viability

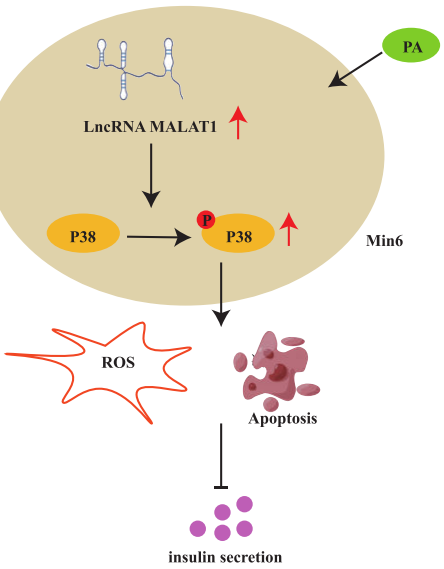

Fig. 6 LncRNA MALAT1 can activate the Phospho-p38 signaling pathway, promote PA-induced ROS and apoptosis in MIN6 cells, and inhibit insulin secretion.

changes mediated by MALAT1. This suggested potential crosstalk between MALAT1 and the MAPK signaling pathway. Based on these findings, we speculated that PA might enhance oxidative stress in cells and activate SP1 to promote the transcription of MALAT1 which, in turn. might further activate the p38 MAPK signaling pathway and increase the generation of ROS. The rise in ROS might lead to oxidative damage to cellular structures, including lipid peroxidation, protein denaturation, and DNA damage, ultimately resulting in cellular dysfunction and apoptosis.

This study also highlighted the potential of MALAT1/Phospho-p38 as therapeutic targets. The results suggested that targeting the MALAT1 or Phospho-p38 signaling pathway could lead to the development of new therapeutic strategies aimed at improving pancreatic β-cell function in patients with T2DM, offering a new direction for T2DM treatment research.

CONCLUSION

This study marked a novel contribution by identifying LncRNA MALAT1 as a critical regulator of the Phospho-p38 signaling pathway, which plays a significant role in promoting ROS production, apoptosis, and inhibition of insulin secretion in PA-induced MIN6 cells. The findings offered new insights into the molecular mechanisms underlying PA-induced pancreatic β-cell dysfunction and suggested that targeting the MALAT1/Phospho-p38 axis could represent a promising therapeutic approach for preserving β-cell function in T2DM patients. This research opens up new avenues for developing interventions aimed at mitigating β-cell destruction in T2DM (Fig. 6).

Appendix A. Supplementary data

Supplementary data associated with this article can be found at https://dx.doi.org/10.2306/scienceasia1513-1874.2025.029.

Acknowledgements: This work was supported by the Opening Project of Yunnan Clinical Medicine Centre (2020LCZXKF-NM02) and the Yunnan Provincial Department of Science and Technology-Kunming Medical University Joint Special Project on Applied Basic Research (202101AY070001-257) and the National Clinical Key Specialty Cultivation Project Platform for Endocrinology(2024NMKFKT-03).

REFERENCES

1. Kumar KK, Aburawi EH, Milos L, Leow MKS, Xu F, Ansari SA, Emerald BS (2024) Exploring histone deacetylases in type 2 diabetes mellitus: pathophysiological insights and therapeutic avenues. *Clin Epigenetics* **16**, 31.
2. Lai SH, Quan Z, Hao Y, Liu J, Wang Z, Dai L, Dai H, He S, et al (2022) Long non-coding RNA LINC01572 promotes hepatocellular carcinoma progression via sponging miR-195-5p to enhance PFKFB4-mediated glycolysis and PI3K/AKT activation. *Front Cell Dev Biol* **9**, 783088.
3. Bajaj G, Singh V, Sagar P, Gupta R, Singhal NK (2024) Phosphoenolpyruvate carboxykinase-1 targeted siRNA promotes wound healing in type 2 diabetic mice by restoring glucose homeostasis. *Int J Biol Macromol* **270**, 132504.
4. Yang Y, Sun M, Yan S, Yao N, Li X, Wu C, Wu Z, Wang F, et al (2024) LINC317.5 as a novel biomarker for hypertriglyceridemia in normal glucose metabolism. *Cell Death Discov* **10**, 194.
5. Chen K, Ou B, Huang Q, Deng D, Xiang Y, HuFang (2024) LncRNA NEAT1 aggravates human microvascular endothelial cell injury by inhibiting the Apelin/Nrf2/HO-1 signalling pathway in type 2 diabetes mellitus with obstructive sleep apnoea. *Epigenetics* **19**, 2293409.
6. Liu R, Wang J, Zhao Y, Zhou Q, Yang X, Gao Y, Li Q, Bai M, et al (2024) Study on the mechanism of modified Gegen Qinlian decoction in regulating the intestinal flora-bile acid-TGR5 axis for the treatment of type 2 diabetes mellitus based on macro genome sequencing and targeted metabonomics integration. *Phytomedicine* **132**, 155329.
7. Gao XR, Sun HZ, Dong WY, Niu JC, Hao SW, Sun HM, Tang GZ, Qi CC, et al (2024) Protective effect of melatonin against metabolic disorders and neuropsychiatric injuries in type 2 diabetes mellitus mice. *Phytomedicine* **131**, 155805.
8. Shi CJ, Zheng YB, Pan FF, Zhang FW, Zhuang P, Fu WM (2021) Gallic acid suppressed tumorigenesis by an LncRNA MALAT1-Wnt/β-Catenin axis in hepatocellular carcinoma. *Front Pharmacol* **12**, 708967.
9. Zhou LJ, Yang DW, Ou LN, Guo XR, Wu BL (2020) Circulating expression level of LncRNA Malat1 in diabetic kidney disease patients and its clinical significance. *J Diabetes Res* **2020**, 4729019.
10. Du P, Wang J, Han Y, Feng J (2020) Blocking the LncRNA MALAT1/miR-224-5p/NLRP3 axis inhibits the hippocampal inflammatory response in T2DM with OSA. *Front Cell Neurosci* **14**, 97.
11. Huang Xm, Li Y, Tong XX, Wu YY, Zhang R, Sheng L, Xu J, Yu ZY, et al (2023) Increased circulating IL-32 is

associated with placenta macrophage-derived IL-32 and gestational diabetes mellitus. *J Clin Endocrinol Metab* **109**, 333–343.
12. Chen CY, Lin MW, Xie XY, Lin CH, Yang CW, Wu PC, Liu DH, Liu CJ, et al (2024) Studying the roles of the renin-angiotensin system in accelerating the disease of high-fat-diet-induced diabetic nephropathy in a db/db and ACE2 double-gene-knockout mouse model. *Int J Mol Sci* **25**, 329.
13. Han Y, Wu N, Xia F, Liu S, Jia DL (2020) Long non-coding RNA GAS5 regulates myocardial ischemia-reperfusion injury through the PI3K/AKT apoptosis pathway by sponging miR-532-5p. *Int J Mol Med* **45**, 858–872.
14. Ni W, Zhang YQ, Zhan ZT, Ye F, Liang YH, Huang J, Chen KL, Chen LH, et al (2023) Correction: A novel lncRNA uc.134 represses hepatocellular carcinoma progression by inhibiting CUL4A-mediated ubiquitination of LATS1. *J Hematol Oncol* **16**, 51.
15. Wu D, Afshari H, Chen L (2024) Pyrroloquinoline quinone mitigates glomerular filtration barrier damages in diabetic mice. *ScienceAsia* 50, 2024072.
16. Liu S, Ma LL, Ren XY, Zhang WL, Shi D, Huo YB, Ba YP, Bai YN, et al (2021) A new mouse model of type 2 diabetes mellitus established through combination of high-fat diet, streptozotocin and glucocorticoid. *Life Sci* **286**, 120062.
17. Weir GC (2019) Glucolipotoxicity, β-Cells, and diabetes: The emperor has no clothes. *Diabetes* **69**, 273–278.
18. Du QQ, Wu XY, Ma K, Ma WW, Liu PW, Hayashi T, Hayashi K, Hattori S, et al (2023) Silibinin alleviates ferroptosis of rat islet β cell INS-1 induced by the treatment with palmitic acid and high glucose through enhancing PINK1/parkin-mediated mitophagy. *Arch Biochem Biophys* **743**, 109644.
19. Yang P, Gao SL, Shen JL, Liu T, Lu K, Han XL, Wang J, Ni HM, et al (2024) TRIM21-mediated ubiquitination of SQSTM1/p62 abolishes its Ser403 phosphorylation and enhances palmitic acid cytotoxicity. *Autophagy* **21**, 178–190.
20. Hirata T, Kawai T, Hirose H, Tanaka K, Tanaka H, Fujii C, Fujita H, Seto Y, et al (2015) Palmitic acid-rich diet suppresses glucose-stimulated insulin secretion (GSIS) and induces endoplasmic reticulum (ER) stress in pancreatic islets in mice. *Endocr Res* **41**, 8–15.
21. Liu X, Zeng X, Chen X, Luo R, Li L, Wang C, Liu J, Cheng J, et al (2019) Oleic acid protects insulin-secreting INS-1E cells against palmitic acid-induced lipotoxicity along with an amelioration of ER stress. *Endocrine* **64**, 512–524.
22. Feng X, Duan H, Li S (2017) Protective role of Pollen Typhae total flavone against the palmitic acid-induced impairment of glucose-stimulated insulin secretion involving GPR40 signaling in INS-1 cells. *Int J Mol Med* **40**, 922–930.
23. Marafie S, Al-Shawaf E, Abubaker J, Arefanian H (2019) Palmitic acid-induced lipotoxicity promotes a novel interplay between Akt-mTOR, IRS-1, and FFAR1 signaling in pancreatic β-cells. *Biol Res* **52**, 44.
24. Ke M, He G, Wang H, Cheng S, Xu Y (2021) Sigma receptor knockdown augments dysfunction and apoptosis of beta cells induced by palmitate. *Exp Biol Med* **246**, 1491–1499.
25. Cruz B, Flores R, Uribe K, Espinoza E, Spencer C, Serafine K, Nazarian A, O'Dell L (2019) Insulin modulates the strong reinforcing effects of nicotine and changes in insulin biomarkers in a rodent model of diabetes. *Neuropsychopharmacol* **44**, 1141–1151.
26. Su Y, Wu H, Pavlosky A, Zou L, Deng X, Zhang Z, Jevnikar A (2016) Regulatory non-coding RNA: new instruments in the orchestration of cell death. *Cell Death Dis* **7**, e2333.
27. Radhakrishnan R, Kowluru R (2021) MALAT1Long non-coding RNA and regulation of the antioxidant defense system in diabetic retinopathy. *Diabetes* **70**, 227–239.
28. Tan A, Li T, Ruan L, Yang J, Luo Y, Li L, Wu X (2021) Knockdown of Malat1 alleviates high-glucose-induced angiogenesis through regulating miR-205-5p/VEGF-A axis. *Exp Eye Res* **207**, 108585.
29. Zhu S, Chen Y, Ye H, Wang B, Lan X, Wang H, Ding S, He X (2022) Circ-LARP1B knockdown restrains the tumorigenicity and enhances radiosensitivity by regulating miR-578/IGF1R axis in hepatocellular carcinoma. *Ann Hepatol* **27**, 100678.
30. Li T, Huang X, Yue Z, Meng L, Hu Y (2020) Knockdown of long non-coding RNA Gm10804 suppresses disorders of hepatic glucose and lipid metabolism in diabetes with non-alcoholic fatty liver disease. *Cell Biochem Funct* **38**, 839–846.
31. Watanabe C, Shibuya H, Ichiyama Y, Okamura E, Tsukiyama-Fujii S, Tsukiyama T, Matsumoto S, Matsushita J, et al (2022) Exocyst complex component 3-like 2 essential roles of on cardiovascular development in mice. *Life (Basel, Switzerland)* **12**, 24189–24199.
32. Chang W, Li W, Li P (2023) The anti-diabetic effects of metformin are mediated by regulating long non-coding RNA. *Fron Pharmacol* **14**, 1256705.
33. Paredes DI, Bello NR, Capasso JE, Procopio R, Levin AV (2023) Mutations in AGBL5 associated with Retinitis pigmentosa. *Ophthalmic Genet* **45**, 275–280.
34. Langner E, Langner T, Kefaloyianni E, Gluck C, Wang BL, Mahjoub MR (2024) Cep120 is essential for kidney stromal progenitor cell growth and differentiation. *EMBO Rep* **25**, 428–454.
35. Zeng Q, Jiang T, Wang J (2024) Role of LMO7 in cancer (Review). *Oncol Rep* **52**, 117.
36. Helmuth G, Susann K, Arne I, Romeo R (2010) MAPK signalling in cellular metabolism: stress or wellness? *EMBO Rep* **11**, 834–840.
37. Mao Y, Wang J, Yu F, Li Z, Li H, Guo C, Fan X (2016) Ghrelin protects against palmitic acid or lipopolysaccharide-induced hepatocyte apoptosis through inhibition of MAPKs/iNOS and restoration of Akt/eNOS pathways. *Biomed Pharmacother* **84**, 305–313.
38. Song X, Shao Z, Xu P (2022) Dexmedetomidine promotes cell proliferation and attenuates insulin resistance in high glucose induced trophoblast cells via inactivating the p38 MAPK pathway. *ScienceAsia* **48**, 734–739.
39. Gong W, Zhu G, Li J, Yang X (2018) LncRNA MALAT1 promotes the apoptosis and oxidative stress of human lens epithelial cells via p38MAPK pathway in diabetic cataract. *Diabetes Res Clin Pract* **144**, 314–321.
40. Liu J, Yao J, Li X, Song Y, Wang X, Li Y, Yan B, Jiang Q (2014) Pathogenic role of lncRNA-MALAT1 in endothelial cell dysfunction in diabetes mellitus. *Cell Death Dis* **5**, e1506.

Appendix A. Supplementary data

Table S1 Level of low-density lipoprotein cholesterol (LDL-C), high-density lipoprotein cholesterol (HDL-C), triglycerides (TG), and total cholesterol (TC) in T2DM.

Group	NC	T2DM
LDL-C	0.25 ± 0.06	$0.56 \pm 0.04^{**}$
HDL-C	2.41 ± 0.48	$1.23 \pm 0.06^{**}$
TC	3.32 ± 0.17	$6.37 \pm 0.06^{**}$
TG	1.45 ± 0.13	$2.44 \pm 0.07^{**}$

$^{**}p < 0.01$ vs. NC group.